



Missouri University of Science and Technology  
Scholars' Mine

---

Electrical and Computer Engineering Faculty  
Research & Creative Works

Electrical and Computer Engineering

---

01 Jan 2006

## Modeling of Dielectric Mixtures Containing Conducting Inclusions with Statistically Distributed Aspect Ratio


Marina Koledintseva  
*Missouri University of Science and Technology*

Sandeep K. R. Chandra

Richard E. DuBroff  
*Missouri University of Science and Technology, red@mst.edu*

Robert W. Schwartz  
*Missouri University of Science and Technology*

Follow this and additional works at: [https://scholarsmine.mst.edu/ele\\_comeng\\_facwork](https://scholarsmine.mst.edu/ele_comeng_facwork)

 Part of the [Electrical and Computer Engineering Commons](#), and the [Materials Science and Engineering Commons](#)

---

### Recommended Citation

M. Koledintseva et al., "Modeling of Dielectric Mixtures Containing Conducting Inclusions with Statistically Distributed Aspect Ratio," *Progress in Electromagnetics Research (PIER)*, vol. 66, pp. 213-228, EMW Publishing, Jan 2006.

The definitive version is available at <https://doi.org/10.2528/PIER06110903>

This Article - Journal is brought to you for free and open access by Scholars' Mine. It has been accepted for inclusion in Electrical and Computer Engineering Faculty Research & Creative Works by an authorized administrator of Scholars' Mine. This work is protected by U. S. Copyright Law. Unauthorized use including reproduction for redistribution requires the permission of the copyright holder. For more information, please contact [scholarsmine@mst.edu](mailto:scholarsmine@mst.edu).

## MODELING OF DIELECTRIC MIXTURES CONTAINING CONDUCTING INCLUSIONS WITH STATISTICALLY DISTRIBUTED ASPECT RATIO

M. Y. Koledintseva, S. K. R. Chandra, R. E. DuBroff  
and R. W. Schwartz

University of Missouri-Rolla  
1870 Miner Circle, Rolla, Missouri, 65409-0040, U.S.A.

**Abstract**—An analytical model of composites made of a dielectric base and randomly oriented metal inclusions in the form of nanorods is presented. This model is based on the generalized Maxwell Garnett (MG) mixing rule. In this model, the nanorod particles are modeled as prolate spheroids with a statistically normal distribution of their aspect ratios. It is shown that parameters of the distribution laws affect the frequency characteristics of the composites both at microwave and optical frequencies. The results of computations are represented.

### 1. INTRODUCTION

The Maxwell Garnett mixing rule [1] is the most popular way for homogenization of composites-intrinsically inhomogeneous mixtures of two or more phases, one of which is typically a dielectric base, or host, material. This is a classical model that has been successfully applied for electromagnetic homogenization of different types of mixtures: with three- and two-dimensional random disposition of inclusions, as well as for ordered structures, such as isotropic and anisotropic metamaterials, including those with a negative refraction index [2].

The Maxwell Garnett model applied to multiphase mixtures describes the effective relative permittivity as [3–5],

$$\varepsilon_{ef} = \varepsilon_b + \frac{\frac{1}{3} \sum_{i=1}^n f_i (\varepsilon_i - \varepsilon_b) \sum_{k=1}^3 \frac{\varepsilon_b}{\varepsilon_b + N_{ik} (\varepsilon_i - \varepsilon_b)}}{1 - \frac{1}{3} \sum_{i=1}^n f_i (\varepsilon_i - \varepsilon_b) \sum_{k=1}^3 \frac{N_{ik}}{\varepsilon_b + N_{ik} (\varepsilon_i - \varepsilon_b)}}, \quad (1)$$

where  $\varepsilon_b$  and  $\varepsilon_i$  are the relative permittivities of the base dielectric and inclusions of the  $i$ -th type, respectively;  $f_i$  is the volume fraction occupied by the inclusions of the  $i$ -th type;  $N_{ik}$  are the depolarization factors of the  $i$ -th type of inclusions, and the index  $k = 1, 2, 3$  corresponds to  $x, y$ , and  $z$  Cartesian coordinates. In general, the permittivities of the base material and inclusions may be frequency-dependent.

The MG formulation typically describes sparse mixtures, where there is no multiple scattering on the dipoles of inclusions. The electric field inside ellipsoidal inclusions is assumed to be static and uniform, but the effective permittivity functions include depolarization factors. Thus, if all the ellipsoids are of the same form for a single type of inclusions, that is, having equal axial ratios, with axes  $A_{1,2,3}$  known, then the depolarization factors are calculated as [2, 6, 7],

$$\begin{aligned} N_{i1} &= \int_0^\infty \frac{A_{i1}A_{i2}A_{i3}}{2(s+A_{i1}^2)^{3/2} \cdot (s+A_{i2}^2)^{1/2} \cdot (s+A_{i3}^2)^{1/2}} ds, \\ N_{i2} &= \int_0^\infty \frac{A_{i1}A_{i2}A_{i3}}{2(s+A_{i2}^2)^{3/2} \cdot (s+A_{i1}^2)^{1/2} \cdot (s+A_{i3}^2)^{1/2}} ds, \\ N_{i3} &= \int_0^\infty \frac{A_{i1}A_{i2}A_{i3}}{2(s+A_{i3}^2)^{3/2} \cdot (s+A_{i1}^2)^{1/2} \cdot (s+A_{i2}^2)^{1/2}} ds \end{aligned} \quad (2)$$

where index  $i$  stands for the depolarization factors of the ellipsoids of  $i$ -th type, and indices 1, 2, and 3 correspond to the ellipsoid's axes. The sum of the depolarization factors satisfies the condition

$$N_{i1} + N_{i2} + N_{i3} = 1. \quad (3)$$

The table of depolarization factors for canonical spheroids (spheres, disks, and cylinders) can be found in [4]. For spherical inclusions, all three depolarization factors are equal (1/3), for the spheroidal particles, two of the depolarization factors are equal. Equation (1) allows that within the same composite material, particles can have different depolarization factors. For nanorods considered as prolate spheroids, an appropriate approximation for one of the depolarization factors is  $N_{i1} \approx (1/a)^2 \ln(a)$  [8], while the two other depolarization factors are  $N_{i2} = N_{i3} = (1 - N_{i1})/2$ . Herein,  $a = l/d$  is the aspect ratio of an inclusion of length  $l$  and diameter  $d$ . It should be mentioned that any shape of an inclusion eventually can be approximated by an ellipsoid of the closest effective dimensions [9].

However, in real mixtures it is almost impossible to have a uniform aspect ratio for all inclusions. Technologically, there is always some

statistical distribution of their sizes. This distribution is typically a normal Gaussian distribution. This distribution should be included in the MG formulation and in computations of frequency characteristics of materials.

In a previous paper [5], we have shown that mixtures of randomly oriented nanosize conducting particles at concentrations far below the percolation threshold can still be treated using the MG mixing rule at optical frequencies, but with some corrections. The dielectric properties of the conducting inclusions are described by the complex relative permittivity

$$\varepsilon_i(j\omega) = \varepsilon'_i - j\varepsilon''_i = \varepsilon'_i - j \frac{\sigma_e}{\omega\varepsilon_0}, \quad (4)$$

the real part of which is much smaller than the imaginary part ( $\varepsilon'_i \ll \sigma_e/(\omega\varepsilon_0)$ ). In (4),  $\sigma_e$  is the bulk conductivity of inclusions.

In [5], subtle effects such as the skin effect in conducting inclusions, the Drude frequency dependence of metals, the effect of the mean free path in small-size conducting inclusions, as well as the dimensional resonances, have been incorporated in the MG model. All these effects have a substantial impact on the resulting absorbance characteristics in the optical band. The statistical distribution of the aspect ratio of the inclusions should also influence the optical characteristics of the composites. Even if all the inclusions in the composite designed for operation at optical frequencies have the same d.c. bulk conductivity, the effective conductivity of inclusions with different aspect ratios is different. This means there will be a statistical spread in the effective conductivity of inclusions.

This paper describes a model incorporating the statistical distribution of the inclusion's aspect ratio. The statistical distribution of initial bulk conductivity and angles of orientation are a topic for further analysis.

The structure of the paper is the following. Section 2 describes a mathematical model of the composite taking the abovementioned statistical distribution and subtle frequency effects into account. The results of calculations based on this model are presented and discussed in Section 3. The conclusions are summarized in Section 4.

## 2. MATHEMATICAL MODEL

Let us consider the case when aspect ratio of inclusions is statistically distributed in some range ( $a_{\min}, a_{\max}$ ). Typically, the particles of inclusions in mixtures are made of the same metal, e.g., silver, and the conductivity of the latter may be assumed as more or less homogeneous

throughout the conglomerate of particles, so we will not consider the statistical distribution of bulk conductivity at this time.

The effective permittivity (1) can then be rewritten in the form

$$\varepsilon_{ef} = \varepsilon_b + \frac{\frac{1}{3} \int_{a_{\min}}^{a_{\max}} \eta_i \varepsilon_b f_i(a) \sum_{k=1}^3 \frac{1}{1 + \eta_i N_{ik}(a)} da}{1 - \frac{1}{3} \int_{a_{\min}}^{a_{\max}} \eta_i f_i(a) \sum_{k=1}^3 \frac{1}{1 + \eta_i N_{ik}(a)} da}. \quad (5)$$

In (5), the volume fraction of the  $i$ -th type inclusions  $f_i(a)$  is calculated as

$$f_i(a) = n_{\Sigma} v_i(a) p(a). \quad (6)$$

The volume fraction of inclusions  $f_i(a)$  is dimensionless and proportional to the volume of inclusions  $v_i(a)$  and the total concentration of inclusions  $n_{\Sigma}$ , defined as a number of inclusions per unit volume of the mixture. In (6),  $p(a)$  is described by the Gaussian distribution law with respect to the aspect ratio [10],

$$p(a) = \frac{1}{\sqrt{2\pi}\sigma_a} e^{-\frac{(a-a_0)^2}{2\sigma_a^2}}, \quad (7)$$

In (7), the mean value is  $a_0$ , and the standard deviation for the values of aspect ratio is  $\sigma_a$ . The volume of a cylindrical inclusion is

$$v_i(a) = \frac{\pi}{4} a d^3. \quad (8)$$

The coefficient  $\eta_i$  in (5) is complex and frequency-dependent in the general case, since it is defined as

$$\eta_i = \frac{\varepsilon_i - \varepsilon_b}{\varepsilon_b} = \eta'_i + j\eta''_i. \quad (9)$$

The limits of integration in (5) are chosen in a reasonable way for the Gaussian distribution as

$$\begin{aligned} a_{\min} &= a_0 - 3\sigma_a; \\ a_{\max} &= a_0 + 3\sigma_a. \end{aligned} \quad (10)$$

The coefficient  $\eta_i$  depends on the bulk conductivity of inclusions. If the conductivity of an inclusion particle equals the bulk conductivity (this is true when the size of an inclusion is much greater than the

wave length), then the frequency dependence of the conductivity may be neglected, and the coefficient is

$$\eta_i = \frac{\varepsilon_i}{\varepsilon_b} - 1 = \frac{\varepsilon'_i}{\varepsilon_b} - j \frac{\sigma_e}{\omega \varepsilon_0 \varepsilon_b} - 1. \quad (11)$$

This is the case at microwave frequencies. However, at optical frequencies, the conductivity of inclusions is frequency-dependent in principle, since subtle frequency-dependent effects, such as skin effect, Drude effect, as well as dimensional resonances in inclusions should be taken into account [5]. Then, the total conductivity  $\sigma_\Sigma$  should replace  $\sigma_e$  in (11), where

$$\sigma_\Sigma = \sigma_D + \sigma_{skin} + \sigma_{res}. \quad (12)$$

In (12),  $\sigma_D$  is the Drude conductivity (see Eq. (12) in [5]), and  $\sigma_{skin}$  is the corrected conductivity that includes both the skin effect in conducting inclusions and the mean free path of electrons (see Eqs. (4)–(8) in [5]).

$$\begin{aligned} \sigma_{skin} &= \sigma_e \cdot \frac{1 - j J_1((1+j)\Delta)}{\Delta J_0((1+j)\Delta)}, \\ \Delta &= \frac{d}{2\delta_{skin}} = \frac{d}{2} \sqrt{\frac{\omega \mu_a \Lambda_{free} \sigma_e}{2}}, \end{aligned} \quad (13)$$

where  $J_0$  and  $J_1$  are the zero and first order Bessel functions of the first kind,  $\Lambda_{free}$  is the coefficient related to the mean free path of electrons, and  $\mu_a = \mu_0 \mu_r$  is the permeability of inclusions (if they are non-magnetic, then  $\mu_a = \mu_0 = 4\pi \cdot 10^{-7}$  H/m). The conductivity  $\sigma_{res}$  is the conductivity term accounting for the dimensional resonance in the inclusion particles (see Eq. (23) in [5]),

$$\sigma_{res} = \frac{4}{\pi} \cdot \frac{l_{ef}^2}{d^2 l} \cdot \frac{f_i(a)}{Z_{in}(a)}, \quad (14)$$

where  $Z_{in}(a)$  represents the complex input impedance of an equivalent “dipole antenna”, corresponding to an inclusion (it is a function of an aspect ratio), and  $l_{ef}$  is its effective dipole antenna length.

The total conductivity (12) is complex:

$$\sigma_\Sigma = \sigma'_\Sigma + j\sigma''_\Sigma. \quad (15)$$

The imaginary part,  $\sigma''_\Sigma$ , contributes to the real part of  $\varepsilon_i$ , and, hence, to the real part of  $\eta_i$ . The real part  $\sigma'_\Sigma$  affects the imaginary part of  $\varepsilon_i$ , and, hence, the imaginary part of  $\eta_i$ .

At microwave frequencies, the conductivity of inclusions can be modeled as the bulk conductivity of the material of inclusions without any frequency-dependent effects. At the same time, for practical manufactured composites (e.g., carbon-filled composites), the distribution of conductivity throughout the conglomerate of particles might extend over a substantial range of conductivity values. In such cases, the effective permittivity of the composite can be calculated through a double Gaussian distribution including both aspect ratio and d.c. bulk conductivity as

$$\varepsilon_{ef} = \varepsilon_b + \frac{\frac{1}{3} \int_{\sigma_{e \min}}^{\sigma_{e \max}} \int_{a_{\min}}^{a_{\max}} \eta_i(\sigma_e) \varepsilon_b f_i(a, \sigma_e) \sum_{k=1}^3 \frac{1}{1 + \eta_i(\sigma_e) N_{ik}(a)} d\sigma_e da}{1 - \frac{1}{3} \int_{\sigma_{e \min}}^{\sigma_{e \max}} \int_{a_{\min}}^{a_{\max}} \eta_i(\sigma_e) f_i(a, \sigma_e) \sum_{k=1}^3 \frac{N_{ik}(a)}{1 + \eta_i(\sigma_e) N_{ik}(a)} d\sigma_e da}, \quad (16)$$

where  $\eta_i(\sigma_e)$  is a function of the bulk conductivity. The volume fraction of the inclusions can be generalized to

$$f_i(a, \sigma_e) = n_{\Sigma} v_i(a) p(a, \sigma_e), \quad (17)$$

and the probability density for the double normal distribution of two statistically independent values, calculated according to [8], is

$$p(a, \sigma_e) = \frac{1}{2\pi\sigma_{cond}\sigma_a} e^{-\frac{(\sigma_e - \sigma_{e0})^2}{2\sigma_{cond}^2} - \frac{(a - a_0)^2}{2\sigma_a^2}}, \quad (18)$$

$\sigma_{cond}$  is the standard deviation for the values of bulk conductivity  $\sigma_e$ , and  $\sigma_{e0}$  is the mean value.

### 3. RESULTS OF COMPUTATIONS

A Matlab program has been developed to calculate reflection and transmission coefficients from a slab of composite material containing metal particles (nanorods) with a statistical distribution of aspect ratio. The program takes into account subtle frequency-dependent effects at optical frequencies, described in [5]. Most of the results shown take into account dimensional resonances in inclusions; however, a few figures (e.g., Figure 2) do not — for comparison reasons.

For the following results, absorbance is defined as  $A = \log_{10}(P_{transm}/P_{incident})$  [bels] and is plotted as a function of wavelength.

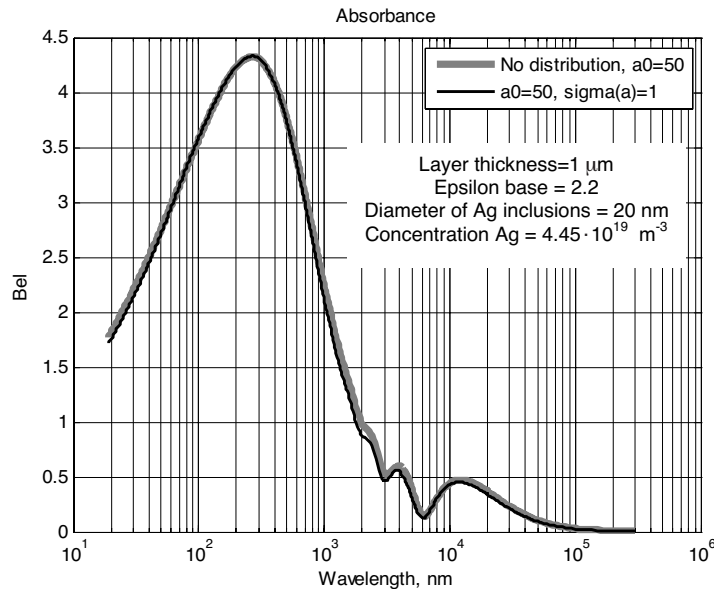


**Figure 1.** Absorbance of a composite with a Gaussian distribution of aspect ratio and with homogeneous aspect ratio. Dimensional resonances are taken into account.

Figure 1 shows that the absorbance curves obtained for inclusions with a homogeneous aspect ratio of  $a_0 = 50$  (lighter curve) and for inclusions having a very narrow distribution curve around  $a_0 = 50$  with a standard deviation of  $\sigma_a = 1$  (dark curve) almost overlap. This suggests that the results for a very narrow distribution of aspect ratios converges to the result for a case of uniform aspect ratios, as expected. In these calculations it was assumed that the mixture contains silver inclusions in a dielectric base. As is mentioned in [5], the frequency-independent permittivity  $\varepsilon_b = 2.2$  can be a good approximation for the PMMA (polymethylmethacrylate) base material in the wave length range of interest. The concentration of Ag particles (number of particles per cubic meter) is constant at  $4.45 \cdot 10^{19} \text{ m}^{-3}$ . This means that the volumetric fraction of inclusions varies, depending on their length and diameter.

Figure 2 shows the effect of including the dimensional resonances into the electromagnetic model of a composite with Gaussian distribution of the aspect ratio. The aspect ratio of Ag inclusions is statistically distributed for both curves, so that the mean aspect ratio is  $a_0 = 50$ , and the standard deviation is  $\sigma_a = 10$ . The



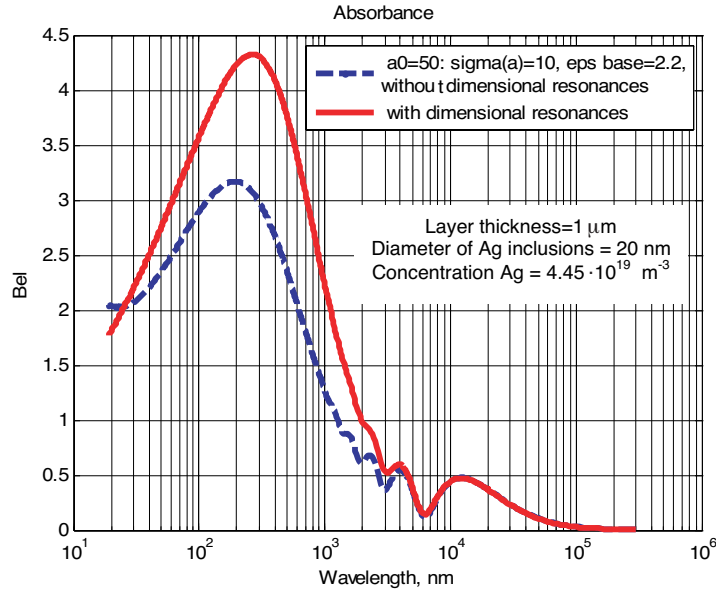


**Figure 2.** Absorbance for two cases: when dimensional resonances are taken into account (solid line) and not taken into account (dashed line).

dielectric base is non-dispersive with a relative permittivity of  $\varepsilon_b = 2.2$ . The concentration of Ag particles is  $4.45 \cdot 10^{19} \text{ m}^{-3}$ . Taking dimensional resonance into account shifts the wavelength of the maximum absorption to the longer wavelengths, and results in a higher absorbance.

The effect of the mean aspect ratio, varying from  $a_0 = 50$  to  $a_0 = 100$ , on the absorbance, with a constant standard deviation  $\sigma_a = 5$  and the diameter of inclusions kept constant at 10 nm, is shown in Figure 3. The higher the aspect ratio, the greater absorbance is, and the relative width of the absorbance curve becomes narrower. In this figure, the dimensional resonances in inclusions are taken into account. There is also a noticeable shift of the maximum absorption peak with the increase of the mean aspect ratio. For the curves in Figure 4, the standard deviation is the same ( $\sigma_a = 10$ ), and the diameter of the inclusions is kept at 20 nm, that is, greater than in Figure 3, and this results in higher maximum absorption than in Figure 3. However, the peak absorption has moved to shorter wavelengths in comparison to the results shown in Figure 3.

In Figure 5, the mean aspect ratio is kept the same for all

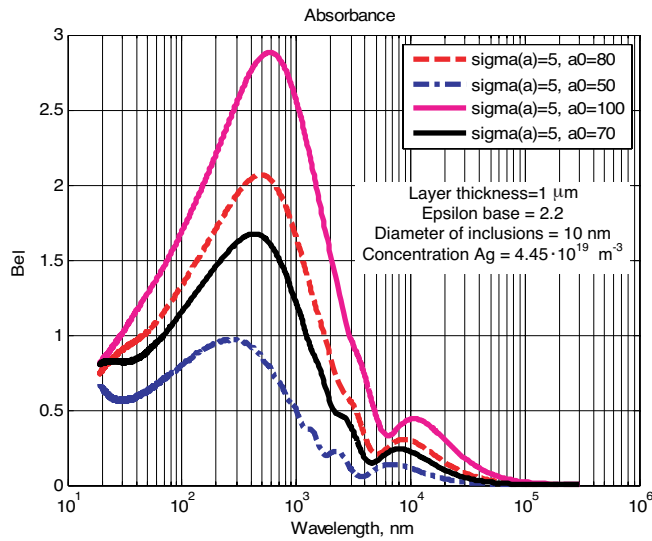


**Figure 3.** The effect of the mean aspect ratio (at the standard deviation  $\sigma_a = \text{const} = 5$ ) on the absorbance of a composite with Gaussian distribution of aspect ratio.

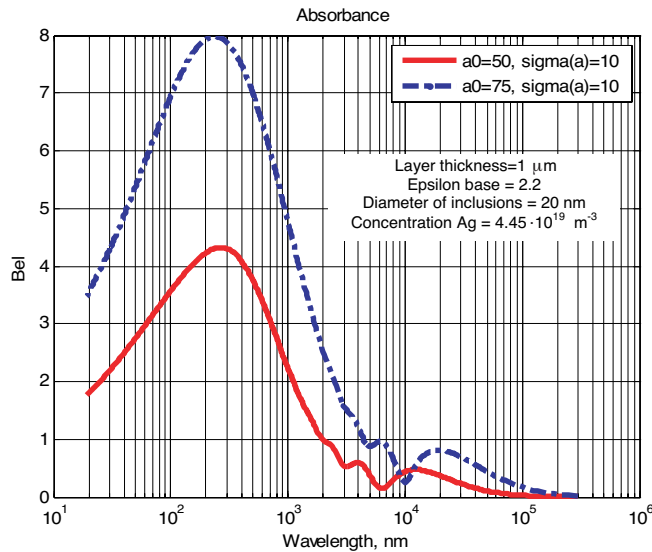


**Figure 4.** The effect of the mean aspect ratio (at the standard deviation  $\sigma_a = \text{const} = 10$ ) on the absorbance of a composite with a Gaussian distribution of aspect ratio.

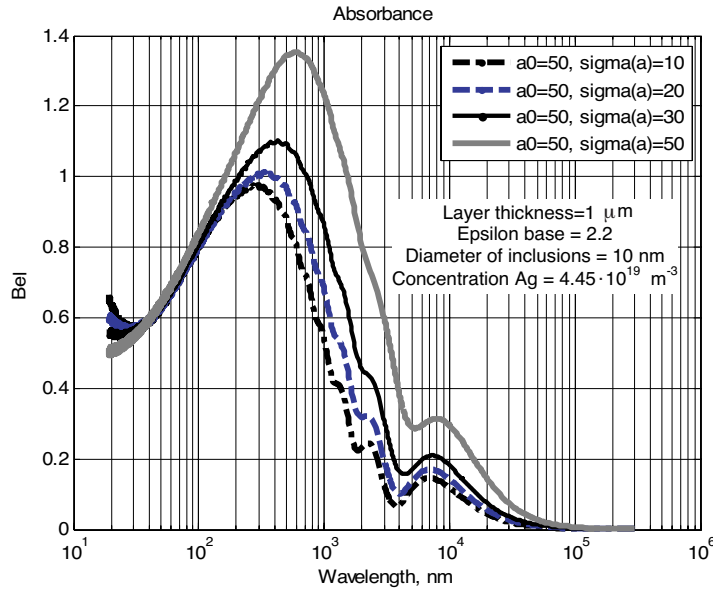


**Figure 5.** The effect of the standard deviation (at  $a_0 = \text{const} = 50$ ) on the absorbance of a composite with a Gaussian distribution of aspect ratio.

the graphs ( $a_0 = 50$ ), the diameter of inclusions is  $d = 10$  nm, and the standard deviation varies. As expected, when the Gaussian distribution curve becomes wider, the width of the absorption curve also increases. In these computations, the absorption peak moves towards the longer wavelengths as  $\sigma_a$  increases. The widening of the curves is asymmetrical. This probably is related to both the increased skin-effect loss at lower frequencies in the thinner inclusions (i.e., with higher aspect ratio) and dimensional resonances. In thicker inclusions (with lower aspect ratio) the trend to the absorption at shorter wavelengths should dominate, but skin-effect loss should be less important.

As in the case of Figure 5, Figure 6 shows that a higher the standard deviation corresponds to a wider absorption curve ( $a_0 = 70$ ,  $d = 10$ ). Because of the higher mean aspect ratio ( $a_0$ ), the absorption peaks in Figure 6 are higher than in Figure 5.

Figure 7 demonstrates that even if the values of  $a_0$  and  $\sigma_a$  are chosen to be identical for all the computations, the actual absorption peak value and position with respect to the wavelength depend on the fixed thickness of the inclusions, while the lengths

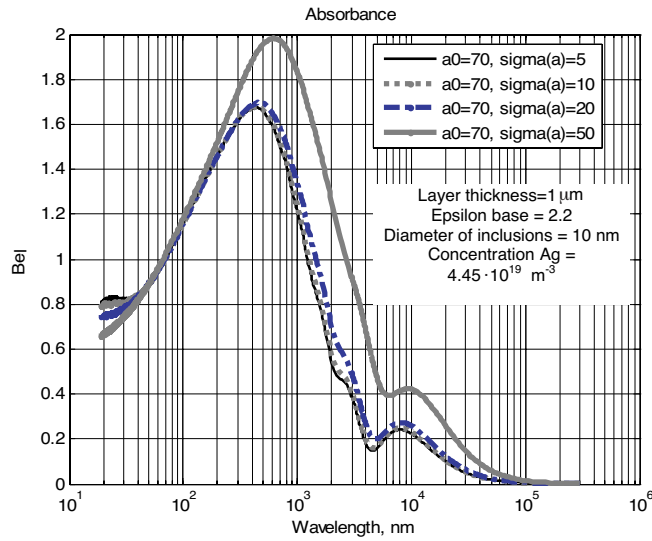


**Figure 6.** The effect of the standard deviation (at  $a_0 = \text{const} = 50$ ) on the absorbance of a composite with a Gaussian distribution of aspect ratio.

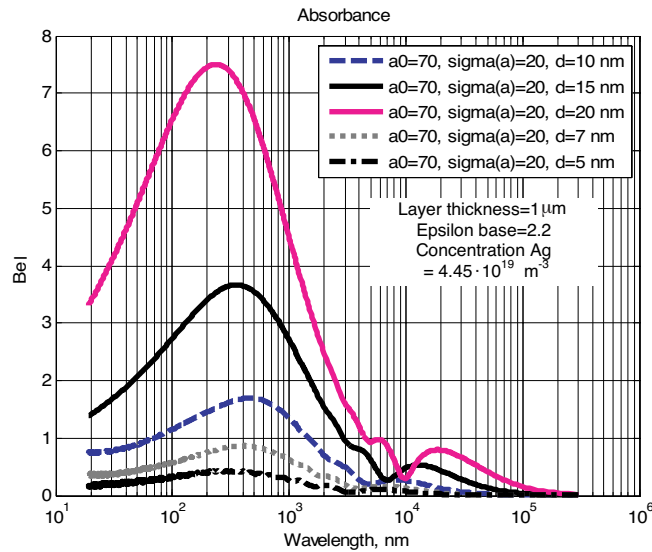


**Figure 7.** The effect of a diameter of inclusions on the absorbance curve, when mean aspect of ratio  $a_0 = \text{const} = 50$  and a standard deviation of  $\sigma_a = 25$  remain the same.

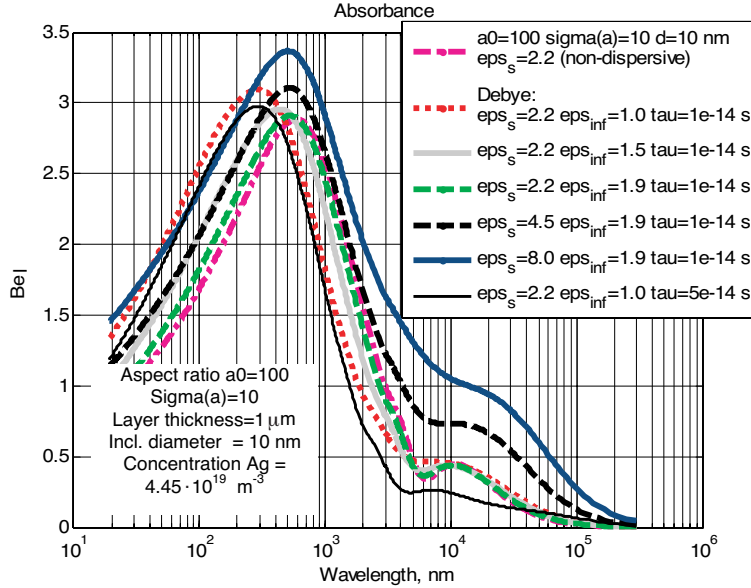


**Figure 8.** The effect of the dispersive (Debye) base material parameters on the absorbance of a composite with a Gaussian distribution of aspect ratio. The concentration of Ag particles is constant at  $4.45 \cdot 10^{19} \text{ m}^{-3}$ .

are statistically distributed. The maximum absorption increases with increasing inclusion diameter, since the corresponding volume fraction of inclusions in the mixture increases — this is an obvious result. As for the position of the absorption peak, when  $d < 10 \text{ nm}$ , increasing  $d$  shifts the absorbance peak to longer wavelengths. When  $d > 10 \text{ nm}$  further increases in  $d$  shift the absorption peak to the shorter wavelengths. This effect might be explained by the combination of two tendencies. Skin effect loss is high, when  $d$  is small and frequencies are low (corresponding to longer wavelengths). At the same time, when  $d$  is small, the mean value of the inclusion length  $l_0$ , corresponding to  $a_0 = \text{const}$ , is also small, and the dimensional resonance shifts to the higher frequencies. This agrees with the graphs in [5, Figure 6].

The effect of the dielectric base material parameters on the absorption curve of the composite is shown in Figures 8 and 9. In Figure 8, the base material is non-dispersive or following the Debye dispersion law,

$$\varepsilon_b = \varepsilon_\infty + \frac{\varepsilon_s - \varepsilon_\infty}{1 + j\omega\tau}, \quad (19)$$

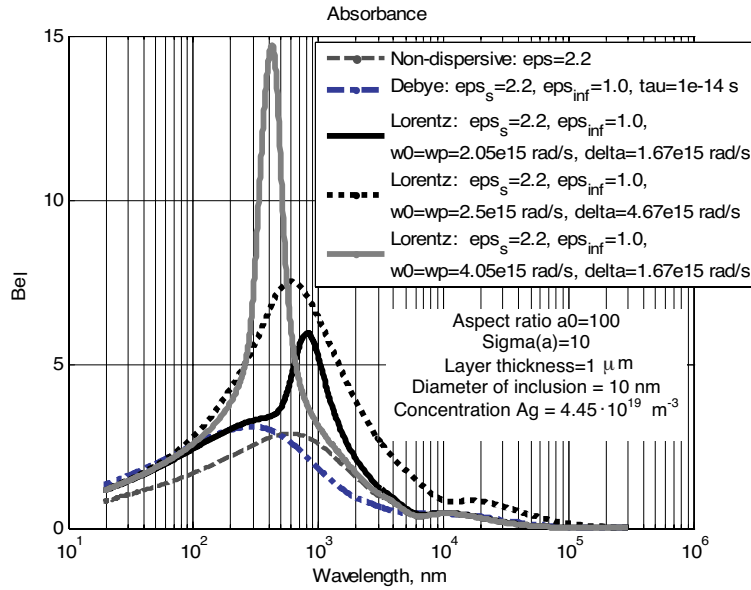


**Figure 9.** The effect of the base material parameters on the absorbance of a composite with a Gaussian distribution of aspect ratio.

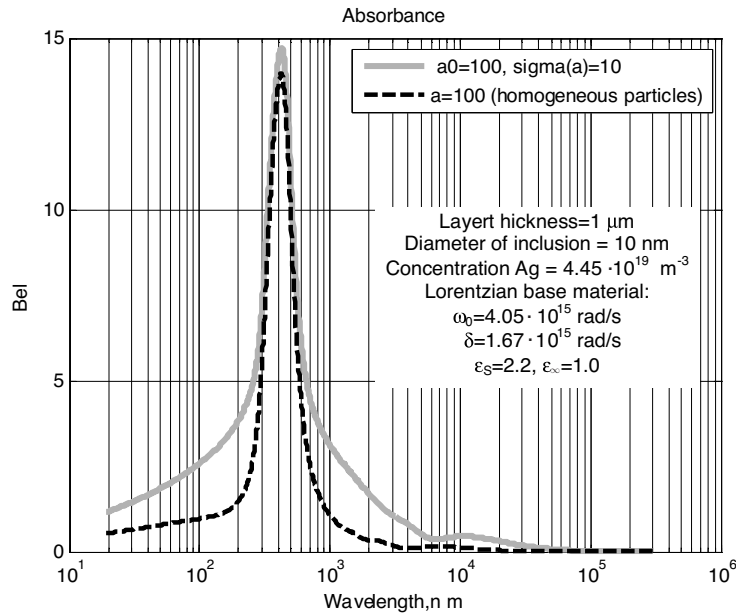
with different parameters for the static permittivity  $\epsilon_s$ , “optical limit” permittivity  $\epsilon_\infty$ , and the Debye relaxation constant  $\tau$ . It is seen that, depending on the parameters of the base material, the resulting curve becomes wider or narrower, the peak of maximum absorption shifts, and the maximum absorption level may increase or decrease. When  $\epsilon_s$  for the base material remains the same, but  $\epsilon_\infty$  increases, there is a trend for the maximum absorption peak to shift to shorter wavelengths. When  $\epsilon_s$  increases (at the same  $\epsilon_\infty$ ), there is almost no shift of the peak, but the peak absorption level increases. The increase of  $\tau$  leads to the shift of the curve to the shorter wavelengths, and the curve becomes wider. However, the relative sensitivity of the curve to the parameters of the dielectric base is not dramatic. Only when  $\epsilon_s$  and the corresponding difference  $(\epsilon_s - \epsilon_\infty)$  is high, will the absorption curve change substantially.

Figure 9 shows absorbance curves for a non-dispersive base material, a Debye material, and three base materials following the Lorentzian frequency law,

$$\epsilon_b = \epsilon_\infty + \frac{(\epsilon_s - \epsilon_\infty)^2 \omega_p^2}{\omega_0^2 - \omega^2 + 2j\omega\delta}. \quad (20)$$

For dielectrics,  $\omega_p = \omega_0$ , that is, the plasma and resonance angular frequencies coincide. The parameter  $(2\delta)$  is the width of the resonance curve at the half magnitude (or  $-3$  dB) level from the maximum. At the same  $\varepsilon_s$  and  $\varepsilon_\infty$ , the increase of  $\delta$  for the Lorentzian dependence leads to the widening of the resultant absorption curve and a decrease in the maximum absorption. When  $\omega_0$  increases, the absorption peak shifts to the shorter wavelengths. These results are quite expected from the material  $Q$ -factor point of view [11].

Figure 10 demonstrates the difference between the absorbance curves obtained when the inclusions are statistically distributed (light solid curve) and statistically uniform (dark dashed line). The base material in each case is the same narrowband Lorentzian. Statistical distribution of the aspect ratio of inclusions makes the absorption curve wider, while the peak value might slightly increase. To form the absorbance curve with more abrupt slopes, it is important to assure that all the inclusions are almost of the same size.



**Figure 10.** Comparison of absorbance curves in presence of a Lorentzian base material for composites with a statistically distributed and a uniform aspect ratio of inclusions.

#### 4. CONCLUSION

An electromagnetic model for a composite material containing nanorods with statistically distributed aspect ratios has been considered. The model is based on the generalized Maxwell Garnett mixing rule for multiphase mixtures. Subtle frequency effects at optical wavelengths are taken into account. The results of computations show that parameters of the distribution law substantially affect the frequency characteristics of the composites at optical frequencies, and it is possible to control the form of the absorbance curve.

#### ACKNOWLEDGMENT

This work was supported by the Air Force Research Laboratory under Contract FA8650-04-C-5704 through the Center for Advanced Materials Technology, University of Missouri-Rolla.

#### REFERENCES

1. Maxwell Garnett, J. C., "Colours in metal glasses and metal films," *Philos. Trans. R. Soc. London, Sect. A.*, Vol. 3, 385–420, 1904.
2. Sihvola, A., "Metamaterials and depolarization factors," *Progress In Electromagnetics Research*, PIER 51, 65–82, 2005.
3. Koledintseva, M. Y., P. C. Ravva, R. E. DuBroff, J. L. Drewniak, K. N. Rozanov, and B. Archambeault, "Engineering of composite media for shields at microwave frequencies," *Proc. IEEE EMC Symposium*, Vol. 1, 169–174, Chicago, IL, August 2005.
4. Koledintseva, M. Y., J. Wu, J. Zhang, J. L. Drewniak, and K. N. Rozanov, "Representation of permittivity for multi-phase dielectric mixtures in FDTD modeling," *Proc. IEEE Symp. Electromag. Compat.*, Vol. 1, 309–314, Santa Clara, CA, Aug. 9–13, 2004.
5. Koledintseva, M. Y., R. E. DuBroff, and R. W. Schwartz, "A Maxwell Garnett model for dielectric mixtures containing conducting particles at optical frequencies," *Progress In Electromagnetics Research*, PIER 63, 223–242, 2006.
6. Landau, L.D., E. M. Lifshitz, and L. P. Pitaevskii, *Electrodynamics of Continuous Media*, 2nd ed., Pergamon, Oxford, New York, 1984.
7. Sihvola, A., *Electromagnetic Mixing Formulas and Applications*, IEE, London, UK, 1999.



8. Lagarkov, A. N. and A. K. Sarychev, "Electromagnetic properties of composites containing elongated conducting inclusions," *Phys. Review B*, Vol. 53, No. 9, 6318–6336, March 1996.
9. Maslovski, S., P. Ikonen, I. Kolmakov, S. A. Tretyakov, and M. Kaunisto, "Artificial magnetic materials based on the new magnetic particle: metasolenoid," *Progress In Electromagnetics Research*, PIER 54, 61–81, 2005.
10. Korn, G. A. and T. M. Korn, *Mathematical Handbook for Scientists and Engineers*, 2nd ed., Chapter 18, McGraw-Hill, 1968.
11. Koledintseva, M. Y., J. L. Drewniak, D. J. Pommerenke, K. N. Rozanov, G. Antonini, and A. Orlandi, "Wideband Lorentzian media in the FDTD algorithm," *IEEE Trans. on Electromag. Compat.*, Vol. 47, No. 2, 392–398, May 2005.